

**Original Article*****In silico* Design of a Vaccine Candidate for SAR S-CoV-2  
Based on Multiple T-cell and B-cell Epitopes****Oso, B. J<sup>1</sup>, Olaoye, I. F<sup>1,2\*</sup>, Ogidi, C. O<sup>3</sup>***1. Department of Biochemistry, McPherson University, Seriki Sotayo, Ogun State, Nigeria**2. Biotechnology Unit, Department of Biological Sciences, Kings University, Odeomu, Nigeria**3. School of Pharmacy and Biomolecular Sciences, Liverpool John Moores University, Liverpool, England*

Received 23 August 2020; Accepted 8 November 2020

Corresponding Author: f.i.olaoeye@ljmu.ac.uk

**Abstract**

Coronaviruses (2019-nCoV) are large single-stranded RNA viruses that usually cause respiratory infections with a crude lethality ratio of 3.8% and high levels of transmissibility. There is yet no applicable clinical evaluation to assess the efficacy of various therapeutic agents that have been suggested as investigational drugs against the viruses despite their respective supposed hypothetical claims due to their antiviral potentials. Moreover, the development of a safe and effective vaccine has been suggested as an intervention to control the 2019-nCoV pandemic. However, a major concern in the development of a 2019-nCoV vaccine is the possibility of stimulating a corresponding immune response without enhancing the induction of the disease and associated side effects. The present investigation was carried out by predicting the antigenicity of the primary sequences of 2019-nCoV structural proteins and identification of B-cell and T-cell epitopes through the Bepipred and PEPVAC servers, respectively. The peptides of the vaccine construct include the selected epitopes based on the VaxiJen score with a threshold of 1.0 and  $\beta$ -defensins as an adjuvant. The putative binding of the vaccine constructs to intracellular toll-like receptors (TLRs) was assessed through molecular docking analysis and molecular dynamics simulations. The selected epitopes for the final vaccine construct are DPNFKD, SPLSLN, and LELQDHNE as B-cell epitopes and EPKLGSLVV, NFKDQVILL, and SSRSSSRSR as T-cell epitopes. The molecular docking analysis showed the vaccine construct could have favorable interactions with TLRs as indicated by the negative values of the computed binding energies. The constructed immunogen based on the immune informatics study could be employed in the strategy to develop potential vaccine candidates against 2019-nCoV.

**Keywords:** 2019-nCoV, Epitope, Immunity, Immunoinformatics, Vaccine**1. Introduction**

Coronaviruses are animal and human viruses that usually cause respiratory infections ranging from mild illnesses, such as the common cold and upper respiratory tract infections to severe diseases, including lethal zoonotic infections, like severe acute respiratory syndrome (SARS) (1, 2). The current virus pandemic, known as COVID-19 or 2019-nCoV, is a large single-stranded RNA virus that includes the surface spike

glycoprotein, lipid-envelope, membrane proteins, and nucleocapsid (3).

The virus is transmitted by respiratory drops with a crude lethality rate of 3.8% which is considerably lower than SARS-CoV (10%) and MERS-CoV (40%), but has higher levels of transmissibility and pandemic risk with an effective reproductive number (R) of 2.9, compared to both SARS-CoV (R=1.77) and MERS-CoV (R<1(4-6)).

Based on the existing indication, the disease presentation varies as some infected individuals are asymptomatic while some generally develop signs and symptoms between the 5th and 6th days after infection (6). It has been documented that the median time from the onset of the disease to recovery could range from 2 to 6 weeks depending on its severity (6).

Airborne precautions, such as hand hygiene, masks, and social distancing are recommended across the globe as non-pharmaceutical control measures to limit the spread of the virus. A variety of therapeutic agents, such as chloroquine, niclosamide, glycyrrhizin, and protease inhibitors, have been suggested as investigational drugs due to their antiviral potentials (7, 8). Despite the purported hypothetical claims of these investigational drugs, there is still no substantive clinical evaluation to assess the efficacy of the drugs aside from the basic fear of unpronounced toxicity.

The development of a safe and effective vaccine has been suggested as a central intervention measure to control the 2019-nCoV pandemic (9). Vaccination success stories include the eradication of infectious diseases, such as smallpox, and the reduction of polio and measles (10). Enjuanes, Dediego (11), (12-14) performed different studies on vaccine candidates, including inactivated whole virus, virus-like particles, and spike protein preparations for the SARS prevention. The main concern to proceed to humans with a SARS-CoV vaccine is the possible induction of enhanced disease and side effects by an inactivated whole virus (15). The structural proteins of SARS-CoV may serve as antigens that could elicit the appropriate immunological reaction upon infection (16, 17).

The present study identified structural antigenic proteins of 2019-nCoV with their respective neutralizing epitopes. Moreover, it developed a fragment-based vaccine through immunoinformatics which could elicit neutralizing antibodies, be safe by not enhancing viral infection, and be employed as a safe vaccine for experimental studies and clinical trials.

## 2. Materials and Methods

### 2.1. Data Retrieval and Structural Analysis

The primary sequence of Glycoprotein, L -protein, Matrix protein, Nucleocapsid protein, Nucleoprotein, and Polymerase in 2019-nCoV were retrieved from the UniProt database (<https://www.uniprot.org/>). Antigenicity prediction of the respective structural proteins was carried out through Vaxijen v2.0 with a 0.5 threshold value (18). The structural protein was selected from each class based on the best antigenic score.

### 2.2. B-Cell Epitope Prediction and Characterization

The Bepipred server (<https://services.healthtech.dtu.dk/service.php?BepiPred-2.0>) was used in linear B-cell epitope prediction. Vaxijen 2.0 server was used for the antigenicity study of chosen epitopes (18) while their respective hypothetical immunogenicity was predicted through the immunogenicity tool of Immune Epitope Database (IEDB) server (<http://tools.iedb.org/>) (19, 20). Toxicity was predicted through the ToxinPred server (<http://crdd.osdd.net/raghava/toxinpred/>) (21). The physicochemical characterization of the respective epitope was predicted using ProtParam Tool on the SIB ExPASy web server ProtParam tool (<https://www.expasy.org/tools/>) using mammalian as the defined organism due to the phylogenetical relationships of mammals with humans (22).

### 2.3. T-Cell Epitope Prediction and Characterization

The PEPVAC web server (<http://immunax.dfci.harvard.edu/PEPVAC/>) was used for the prediction of antigenic major histocompatibility complex(MHC)-Class-I-Restricted T Cell epitopes (9-mer) (23). Vaxijen 2.0 server was used for the antigenicity study of chosen epitopes while their respective hypothetical immunogenicity was predicted through the immunogenicity tool of the IEDB server (<http://tools.iedb.org/>) (19, 20). Toxicity was predicted through the ToxinPred server (<http://crdd.osdd.net/raghava/toxinpred/>) (21). The physicochemical characterization of the respective

epitope was predicted using ProtParam Tool on the SIB ExPASy web server ProtParam tool (<https://www.expasy.org/tools/>) using mammalian as the defined organism (22).

#### 2.4. Estimation of Population Coverage

The human leukocyte antigen (HLA)-alleles distribution among the world population was predicted through the IEDB population coverage analysis tool. This tool is used for the analysis of the potential cytotoxic T lymphocyte and helper T lymphocyte epitopes as well as their MHC binding alleles (<http://tools.iedb.org/>) (19, 20).

#### 2.5. Multi-Epitope Vaccine Construct Design

The selected B-cell and T-cell epitopes were respectively linked with GP GPG and AAY linkers. A 45-amino-acid-length,  $\beta$ -defensin, was selected as the adjuvant. The amino acid sequence of the adjuvant (GIINTLQKYYCRVRGGRCVLSCLPKKEEQIGKC STRGRKCCRRKK) was added to the N-terminal of the vaccine construct using EAAAK as the linker. After the addition of the adjuvant and linkers, the final length of the vaccine candidate was 132 residues.

#### 2.6. Secondary Structure Prediction and Structural Modeling of the Vaccine Construct

The self-optimized prediction method with alignment was used for the prediction of the secondary structure of the vaccine. The i-TASSER server (<https://zhanglab.ccmb.med.umich.edu/I-TASSER/>) was used in modeling the final subunit vaccine tertiary structure (24). The predicted model of the vaccine protein was refined through the GalaxyRefine web server (<http://galaxy.seoklab.org/index.html>). The structural characterization of the vaccine construct was carried out through Qualitative Model Energy Analysis (QMEAN) (25) while the Ramachandran plot was obtained using the PROCHECK server (<https://servicesn.mbi.ucla.edu/PROCHECK/>) (26, 27).

#### 2.7. Molecular Docking between the Vaccine and

#### TL Receptor

The 3D structure of human toll-like receptors (TLR)-3 and TLR-8 obtained from Research Collaboratory for Structural Bioinformatics (RSCB) with RSCBIDs of 2A0Z and 3WN4, respectively, were utilized for further molecular docking studies. The peptide models were docked against TLRs through the HAWKDOCK server tool (<http://cadd.zju.edu.cn/hawkdock/>) (28) and their binding potential was also analyzed. Furthermore, the Molecular Mechanics/Generalized Born Surface Area (MM/GBSA) computations were done to predict the binding free energy of the receptor-vaccine interaction via the HAWKDOCK server (<http://cadd.zju.edu.cn/hawkdock/>). The means of the binding scores between the two receptors were compared using the student's *t*-test.

#### 2.8. Molecular Dynamics Simulation

The assessment of the binding effects of the TLRs on the molecular dynamics of the vaccine construct was performed through iMODS, an internal coordinates normal mode analysis server (<http://imods.chaconlab.org>) (29).

### 3. Results and Discussion

#### 3.1. Data Retrieval and Structural Analysis

The present study focused on the optimization of epitope-based vaccines through computational analyses. The immunogenicity of any vaccine depends on the suitable processing of the antigenic epitopes which are specific immunogenic machinery of the pathogen. In total, 14 sequences of COVID-19 structural proteins were retrieved from the UniProt database. In contrast to whole-cell vaccines, epitope-based vaccines could be favorable in clinical trials due to their cost-effectiveness and non-infectious nature (30). Hypothetically, ORF10 protein, envelope small membrane protein, membrane protein, ORF6 protein, ORF7a protein, ORF8 protein, nucleoprotein, ORF9b protein, and ORF7b protein were predicted to have the

highest antigenicity threshold of 0.5 and were selected for subsequent immunoinformatics study (Table 1).

**Table 1.** Properties of the selected proteins on UniProt

UniProtKB ID	Protein Name	Antigenicity Score	Remark
A0A663DJA2	Hypothetical ORF10 protein	0.7185	Antigen
P0DTC1	Replicase polyprotein 1a (pp1a)	0.4787	Non-antigen
P0DTC2	Spike glycoprotein	0.4646	Non-antigen
P0DTC3	ORF3a protein	0.4945	Non-antigen
P0DTC4	Envelope small membrane protein	0.6025	Antigen
P0DTC5	Membrane protein	0.5102	Antigen
P0DTC6	ORF6 protein	0.6131	Antigen
P0DTC7	ORF7a protein	0.6441	Antigen
P0DTC8	ORF8 protein	0.6502	Antigen
P0DTC9	Nucleoprotein Replicase	0.5059	Antigen
P0DTD1	polyprotein 1ab	0.4624	Non-antigen
P0DTD2	ORF9b protein	0.9060	Antigen
P0DTD3	ORF14 protein	0.4021	Non-antigen
P0DTD8	ORF7b protein	0.8462	Antigen

### 3.2. Properties of the Selected Epitopes

Sequences of the epitope in the proteins with the acceptable antigenicity were identified through

Bepipred and PEPVAC servers and were assumed to be significant in terms of immune response (31, 32). The selected B-cell and T-cell epitopes for the final vaccine construction and their corresponding properties are presented in tables 2 and 3.

The selected epitopes based on the VaxiJen score with a threshold of 1.0 for the final vaccine construct are DPNFKD, SPLSLN, and LELQDHNE listed as B-cell epitopes and EPKLGSLVV, NFKDQVILL, and SSRSSSR listed as T-cell epitopes based on the peptides which can be bound to MHC class I molecules. B-cells have been known to play an indispensable role in the antibody responses elicited from diverse infections and vaccinations. However, the up-regulation of MHC antigen presentation through the TLRs could promote antigen-specific T-cell responses (33). The sequences were predicted from nucleoprotein and ORF9b protein.

Stimulation of immune response with multiple epitopes could lead to marked synergy in the activation of antigen-presenting cells (34). The selected epitopes showed an acceptable extent of immunogenicity and no toxicity; these properties could invariably enhance the functionality of the vaccine construct. The molecular weight of the selected epitopes ranges from 629.79 Da to 1089.44 Da with good antigenic properties. The isoelectric point prediction revealed that the selected B-cell epitopes were acidic while the selected T-cell epitopes were basic.

**Table 2.** Properties of the selected B-cell epitopes for the final vaccine construction

UniProtKB ID	Protein Name	Sequence	VaxiJen score	Immunogenicity score	Prediction	pI	Molecular weight
P0DTC2	Nucleoprotein	DPNFKD	2.88	-0.09	Non-toxin	4.21	734.83
P0DTD2	ORF9b protein	SPLSLN	1.83	-0.18	Non-toxin	5.88	629.79
P0DTD8	ORF7b protein	LELQDHNE	1.45	-0.07	Non-toxin	4.14	997.15

**Table 3.** Properties of the selected T-cell epitopes for the final vaccine construction

UniProtKB ID	Sequence	VaxiJen score	Immuno genicity score	Toxicity	pI	Molecular weight	HLA Class I Alleles
P0DTC8	EPKLGSLVV	1.38	-0.19	Non-Toxin	6.35	941.27	HLA-B*53:01,HLA-B*35:01,HLA-B*07:02,HLA-B*54:01,HLA-B*51:01,HLA-B*51:02
P0DTC9	NFKDQVILL	1.17	-0.02	Non-Toxin	6.19	1089.44	HLA-A*02:01,HLA-A*02:02,HLA-A*02:03,HLA-A*02:04,HLA-A*02:05,HLA-A*02:06,HLA-A*68:02,HLA-A*24:02,HLA-B*38:01
P0DTC9	SSRSSRSR	1.23	-0.52	Non-Toxin	12.31	1009.14	HLA-A*33:01,HLA-A*11:01,HLA-A*31:01,HLA-A*03:01,HLA-A*68:01,HLA-A*66:01

HLA: human leukocyte antigen

### 3.3. Population Coverage Analysis

The population coverage analysis which computes the fraction of individuals, which was predicted to respond to the set of selected T-cell epitopes, suggested that the selected MHC-Class I covers 90.04% of the world population. This information revealed the proper population coverage (Table 4). The highest population coverage based on HLA genotypic frequencies with the assumption of non-linkage disequilibrium between the HLA loci was in East Asia. Moreover, it reached the above-average values in other areas, except in Central America where the lowest coverage was found. This showed minimal complexity in the development of a vaccine with different epitopes (35). The two highest coverages were found in East Asia where the virus first appeared and Europe where several outbreaks occurred (36).

### 3.4. Physicochemical Properties of the Vaccine Construct

The selected antigenic B-cells and T-cells epitopes were considered for the construction of a multi-epitope vaccine using  $\beta$ -defensin as the adjuvant (Figure 1). The final vaccine constructs contained 130 amino acid residues. The results of the predicted antigenicity and physicochemical characterization of the final vaccine construct are presented in table 5. The physicochemical

features and efficiency of any peptide were determined by the unique sequence of the peptide (37, 38). The construct had a molecular weight of 13875.91 Da with good antigenic properties based on the VaxiJen score with a threshold of 0.5. This property revealed the probable immunogenic sufficiency of the construct and its potential to stimulate a response against pathogenic epitopes.

The theoretical isoelectric point value indicated that the vaccine was basic. The estimated half-life in mammalian reticulocytes through *in vitro* investigation was approximately 30 h. However, the construct had a high instability index. The aliphatic index indicated the stability of the construct over a wide range of temperatures. The hydrophilicity of the construct was due to the negative grand average of hydropathicity.

### 3.5. Secondary and Conformational Structures of the Designed Vaccine

Moreover, computational studies were performed on the secondary and conformational structures of the designed vaccine. The predicted secondary structure indicated that alpha-helix, extended strand, beta-turn, and random coil percentages were 16.92%, 26.15%, 6.15%, and 50.77%, respectively, with 22, 34, 8, and 66 amino acid residues, respectively (Figure 2). The GalaxyRefine server refined i-TASSER predicted

tertiary structure leading to an increase in the number of residues in the favored region.

The refined best model with the highest percentage of residues in the most favored region in the Ramachandran plot and SWISSQMEAN was selected for further studies (Figure 3). The Ramachandran plot which presents the most favorable combinations of phi-psi values showed that a total of 103 amino acids were

non-glycine and non-proline residues. Moreover, 63(61.2%), 23(22.3%), 5(4.9%), and 12 (11.7%) residues were found in the most favored regions, additionally allowed regions, generously allowed regions, and disallowed regions, respectively. The glycine (shown as triangles) and proline residues were 16 and 10, respectively. The computed QMEAN score was -7.86.

**Table 4.** World population coverage of the selected T-cell epitopes

Population	Coverage <sup>a</sup>	Average Hit <sup>b</sup>	pc90 <sup>c</sup>
Central Africa	73.21	1.08	0.37
Central America	2.98	0.03	0.1
East Africa	73.16	1.05	0.37
East Asia	94.63	1.77	1.14
Europe	92.69	1.65	1.07
North Africa	80.71	1.26	0.52
North America	91.79	1.63	1.05
Northeast Asia	87.81	1.33	0.82
Oceania	87.78	1.22	0.82
South Africa	71.61	0.99	0.35
South America	82.94	1.22	0.59
South Asia	81.02	1.19	0.53
Southeast Asia	87.46	1.28	0.8
Southwest Asia	79.39	1.2	0.49
West Africa	78.87	1.24	0.47
West Indies	88.68	1.55	0.88
World	90.04	1.51	1
Mean±SD	79.10± 20.24	1.25±0.37	0.67±0.29

<sup>a</sup> Projected population coverage

<sup>b</sup> Average number of epitope hits/human leukocyte antigen combinations recognized by the population

<sup>c</sup> Minimum number of epitope hits/human leukocyte antigen combinations recognized by 90% of the population

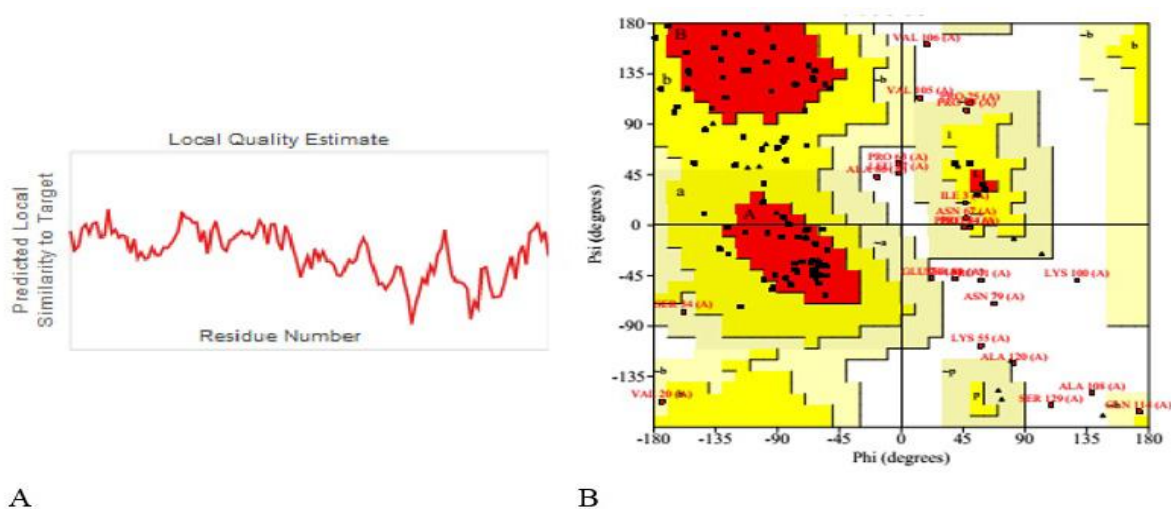


**Figure 1.** (A) Sequence and (B) graphical presentation of the vaccine construct consisting of an adjuvant (purple) at the N-terminal end that is linked to the whole multi-epitope sequence through EAAK linker (blue). B-cell and T-cell epitopes are fused with the help of GPGPG (yellow) and AAY (brown), linkers, respectively.

**Table 5.** Antigenicity and physicochemical properties of the vaccine construct

Molecular weight (Da)	Antigenicity	Theoretical pI	Half-life (h)	Instability index	Aliphatic index	Grand average of hydropathicity index
13875.91	0.6403	9.66	30	43.04	72.08	-0.496

**Figure 2. (A)** Secondary structure of the vaccine construct revealing alpha helix (blue), extended strand (red), beta-turn (green), and random coil (yellow); **(B)** tertiary structure of the multi-epitope vaccine after refinement.





### 3.6. Molecular Docking Analysis

The computational binding affinities through molecular docking studies were carried out through the HAWKDOCK server. The TLRs are single-pass membrane-spanning receptors that play an essential role in the mediation of the immune system (39). They recognize structurally conserved pathogen-associated molecular patterns on a range of pathogens, including viruses leading to the induction of inflammatory reactions mediated via the nuclear factor- $\kappa$ B activation and by interferon.

The TLRs, such as TLR3 and TLR8, located in endosomal compartments have been identified as mediating recognition of viral proteins. They promote the TLR-dependent antiviral immunity leading to innate immune activation as the first line of host defense as well as in adaptive immunity (39, 40). The result of the molecular docking analysis using the HAWKDOCK server revealed that the energy scores for different models and the mean of the first five models with the lowest energy scores were computed as the mean score for each interaction.

The accuracy of the ranking was assessed through MM/GBSA free energy computation through an approximation of the solvent electrostatic contribution in the Poisson-Boltzmann model (41, 42). The obtained results indicated that the reliability in the methods employed with the interaction of the construct with TLR8 has the highest affinity as shown by the least binding energy value between the vaccine construct and the TLR (Table 6). However, model 1 with the lowest HAWKDOCK score was chosen as the best-docked complex of each interaction (Figure 4).

The interactions of the vaccine construct with TLR3 and TLR8 could activate the TLRs. This could subsequently lead to the recruitment of adaptor proteins, such as myeloid differentiation primary response 88. It could activate the nuclear factor- $\kappa$ B and interferons production through sequential activation of IL-1 receptor-associated kinase family kinases, an inhibitor of  $\kappa$ B kinase, and mitogen-activated protein kinase.

This activation cascade could lead to an immune response against the molecular patterns of the vaccine construct (39).

**Table 6.** Mean binding free energy (kcal/mol) of the complex of the vaccine construct with TLR-3 and TLR-8

	TLR-3	TLR-8
Hawkdock Score	-5282.35 $\pm$ 141.29	-6709.91 $\pm$ 255.12*
Molecular Mechanics/Generalized Born Surface Area	-21.12 $\pm$ 0.30	-51.23 $\pm$ 0.13*

\*  $P < 0.05$

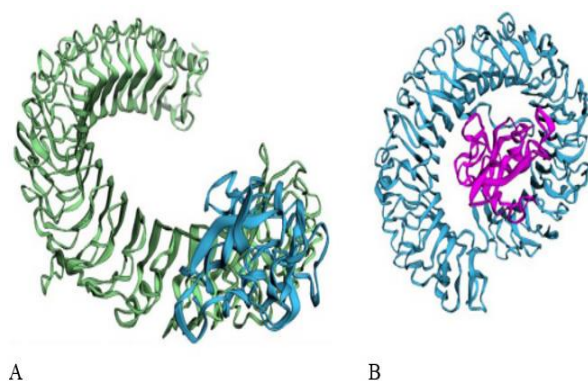


**Figure 4.** Docked complex of vaccine constructs with (A) toll-like receptor 3 (blue) and (B) toll-like receptor 8 (purple).

### 3.7. Molecular Dynamics Simulation

Molecular dynamics study is critically essential for checking the stability of the protein-protein complex in any *in silico* analysis. Protein stability can be determined by comparing essential protein dynamics with their normal modes (43). The stability and flexibility of the docked complexes were assessed through the normal mode analysis using the iMODS server. The results showed that the vaccine construct could modulate the TLR3 and TLR8 structures (Figure 5).

The binding of the vaccine constructs decreased the capability of each of the receptors to deform at each of its residues as shown by the main-chain deformability graph and the experimental B-factor (Figure 5I and II) (44). However, it had a varying effect on the



eigenvalues which represented the motion stiffness of the receptors. The eigenvalues were  $8.74 \times 10^{-6}$  and  $8.77 \times 10^{-5}$  for TLR3 and TLR8, respectively, and  $1.50 \times 10^{-5}$  and  $9.72 \times 10^{-5}$  for the complexes of the vaccine construct with TLR3 and TLR8, respectively (Figure 5 III).

This showed that the interaction of the vaccine constructs increased the energy required to deform the TLR3. However, it decreased the eigenvalue of TLR8 which led to easier deformation. Moreover, the computed eigenvalues had an inverse relationship with the results of the variance associated with each normal mode of the unbound receptors and the complexes

(Figure 5 IV).

Furthermore, the covariance matrix, which indicated coupling between pairs of residues within the receptors, showed that the vaccine constructs lowered the correlation motions in the TLRs as indicated by a decline in the strength of redness (Figure 5 V). Similarly, the elastic network model showed that the interaction of the vaccine constructs reduced the stiffness of the springs that connected the atoms (Figure 5 VI) (29). The binding of vaccine constructs to the TLRs on antigen-presenting cells could lead to the activation of TLRs and induce an inflammatory response that could elicit acquired immunity (45).

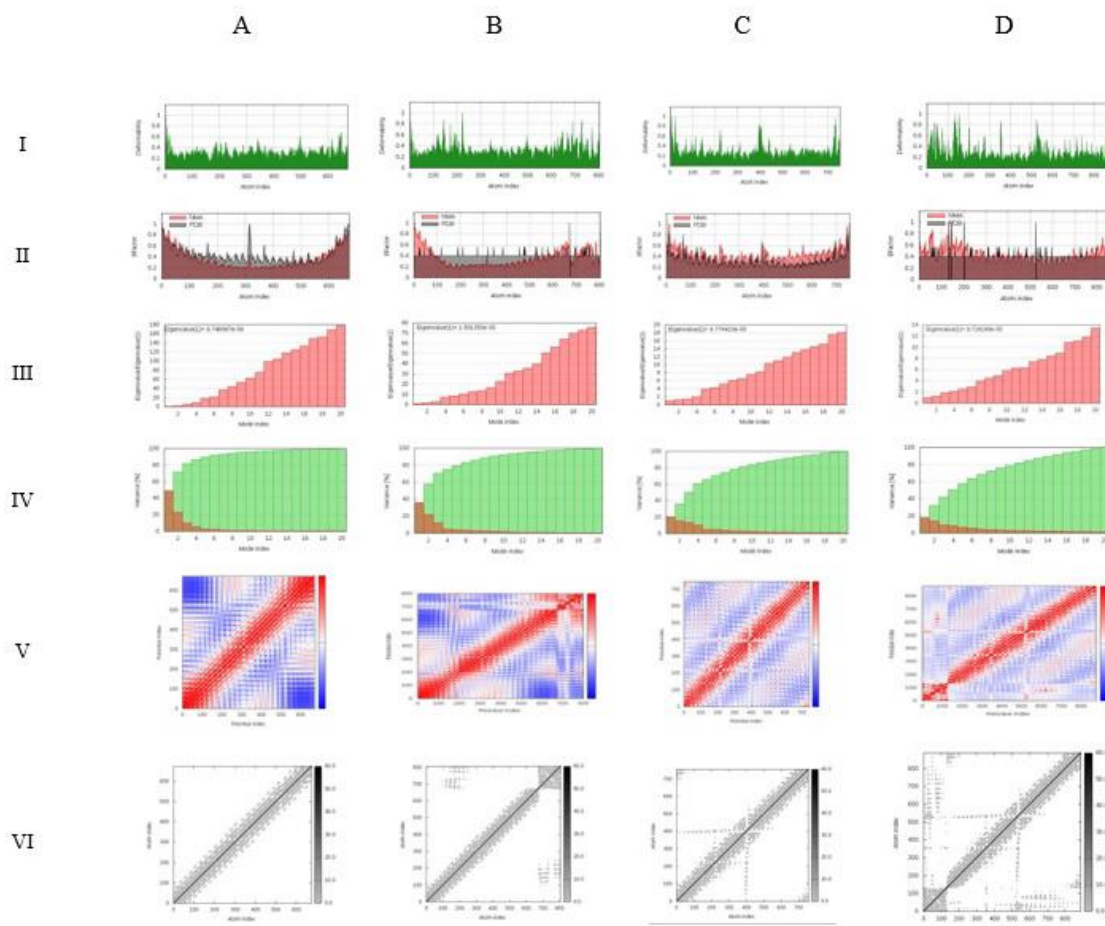


**Figure 6.** Molecular dynamics simulation of (A) toll-like receptor 3, (B) the docked complex of Toll-like receptor 3 with the vaccine construct, (C) toll-like receptor 8, and (D) toll-like receptor 8 with the vaccine construct showing the (I) main-chain deformability, (II) experimental B-factor, (III) eigenvalues, (IV) variance associated to each normal mode, (V) covariance matrix, and (VI) The elastic network model.

#### 4. Conclusion

The presentation of this epitope-based vaccine construct based on the antigenic epitopes of the structural proteins of 2019-nCoV could be harnessed to activate TLR3 and TLR8 signaling. This could therapeutically elicit appropriate vaccine-specific immunological responses from 2019-nCoV infection.

#### Authors' Contribution

Study concept and design: B. J. O., I. F. O. and C. O. O.

Acquisition of data: B. J. O., I. F. O. and C. O. O.

Analysis and interpretation of data: B. J. O.

Drafting of the manuscript: B. J. O. and I. F. O.

Critical revision of the manuscript for important intellectual content: B. J. O., I. F. O. and C. O. O.

Statistical analysis: None

Administrative, technical, and material support: B. J. O., I. F. O. and C. O. O.

#### Conflict of Interest

The authors declare that they have no conflict of interest.

#### Grant Support

The current research was not financially supported by any institute or person.

#### References

1. Korsman SNJ, van Zyl GU, Nutt L, Andersson MI, Preiser W. Human coronaviruses. In: Korsman SNJ, van Zyl GU, Nutt L, Andersson MI, Preiser W, editors. *Virology*. Edinburgh: Churchill Livingstone; 2012. p. 94-5.
2. Ye ZW, Yuan S, Yuen KS, Fung SY, Chan CP, Jin DY. Zoonotic origins of human coronaviruses. *Int J Biol Sci*. 2020;16(10):1686-97.
3. Wu C, Liu Y, Yang Y, Zhang P, Zhong W, Wang Y, et al. Analysis of therapeutic targets for SARS-CoV-2 and discovery of potential drugs by computational methods. *Acta Pharm Sin B*. 2020;10(5):766-88.
4. Chen J. Pathogenicity and transmissibility of 2019-nCoV-A quick overview and comparison with other emerging viruses. *Microbes Infect*. 2020;22(2):69-71.
5. Liu T, Hu J, Xiao J, He G, Kang M, Rong Z, et al. Time-varying transmission dynamics of Novel Coronavirus Pneumonia in China. *BioRxiv*. 2020:2020.01.25.919787.
6. WHO. Coronavirus disease 2019 (COVID-19): situation report, 73. Geneva: World Health Organization; 2020 2020-04-02.
7. Cinatl J, Morgenstern B, Bauer G, Chandra P, Rabenau H, Doerr HW. Glycyrrhizin, an active component of liquorice roots, and replication of SARS-associated coronavirus. *Lancet*. 2003;361(9374):2045-6.
8. Wu C-J, Jan J-T, Chen C-M, Hsieh H-P, Hwang D-R, Liu H-W, et al. Inhibition of severe acute respiratory syndrome coronavirus replication by niclosamide. *Antimicrob Agents Chemother*. 2004;48(7):2693-6.
9. Dhama K, Sharun K, Tiwari R, Dadar M, Malik YS, Singh KP, et al. COVID-19, an emerging coronavirus infection: advances and prospects in designing and developing vaccines, immunotherapeutics, and therapeutics. *Hum Vaccin Immunother*. 2020;16(6):1232-8.
10. Greenwood B. The contribution of vaccination to global health: past, present and future. *Philos Trans R Soc Lond B Biol Sci*. 2014;369(1645):20130433.
11. Enjuanes L, Dediego ML, Alvarez E, Deming D, Sheahan T, Baric R. Vaccines to prevent severe acute respiratory syndrome coronavirus-induced disease. *Virus Res*. 2008;133(1):45-62.
12. Lamirande EW, DeDiego ML, Roberts A, Jackson JP, Alvarez E, Sheahan T, et al. A live attenuated severe acute respiratory syndrome coronavirus is immunogenic and efficacious in golden Syrian hamsters. *J Virol*. 2008;82(15):7721-4.
13. Lokugamage KG, Yoshikawa-Iwata N, Ito N, Watts DM, Wyde PR, Wang N, et al. Chimeric coronavirus-like particles carrying severe acute respiratory syndrome coronavirus (SCoV) S protein protect mice against challenge with SCoV. *Vaccine*. 2008;26(6):797-808.
14. Zhou Z, Post P, Chubet R, Holtz K, McPherson C, Petric M, et al. A recombinant baculovirus-expressed S glycoprotein vaccine elicits high titers of SARS-associated coronavirus (SARS-CoV) neutralizing antibodies in mice. *Vaccine*. 2006;24(17):3624-31.
15. Perlman S, Dandekar AA. Immunopathogenesis of coronavirus infections: implications for SARS. *Nat Rev Immunol*. 2005;5(12):917-27.
16. Lu X, Chen Y, Bai B, Hu H, Tao L, Yang J, et al. Immune responses against severe acute respiratory syndrome coronavirus induced by virus-like particles in

- mice. *Immunology*. 2007;122(4):496-502.
17. Walls AC, Park YJ, Tortorici MA, Wall A, McGuire AT, Veesler D. Structure, Function, and Antigenicity of the SARS-CoV-2 Spike Glycoprotein. *Cell*. 2020;181(2):281-92 e6.
  18. Doytchinova IA, Flower DR. VaxiJen: a server for prediction of protective antigens, tumour antigens and subunit vaccines. *BMC Bioinform*. 2007;8:4.
  19. Larsen JEP, Lund O, Nielsen M. Improved method for predicting linear B-cell epitopes. *Immun Res*. 2006;2(1):1-7.
  20. Ponomarenko JV, Bourne PE. Antibody-protein interactions: benchmark datasets and prediction tools evaluation. *BMC Struct Biol*. 2007;7(1):1-19.
  21. Gupta S, Kapoor P, Chaudhary K, Gautam A, Kumar R, Open Source Drug Discovery C, et al. In silico approach for predicting toxicity of peptides and proteins. *PLoS One*. 2013;8(9):e73957.
  22. Artimo P, Jonnalagedda M, Arnold K, Baratin D, Csardi G, de Castro E, et al. ExPASy: SIB bioinformatics resource portal. *Nucleic Acids Res*. 2012;40:W597-603.
  23. Reche PA, Reinherz EL. PEPVAC: a web server for multi-epitope vaccine development based on the prediction of supertypic MHC ligands. *Nucleic Acids Res*. 2005;33:W138-42.
  24. Yang J, Zhang Y. I-TASSER server: new development for protein structure and function predictions. *Nucleic Acids Res*. 2015;43(W1):W174-81.
  25. Benkert P, Biasini M, Schwede T. Toward the estimation of absolute quality of individual protein structure models. *Bioinformatics*. 2011;27:343-50.
  26. Laskowski RA, MacArthur MW, Moss DS, Thornton JM. PROCHECK: a program to check the stereochemical quality of protein structures. *J Appl Crystallogr*. 1993;26(2):283-91.
  27. Laskowski RA, Rullmann JAC, MacArthur MW, Kaptein R, Thornton JM. AQUA and PROCHECK-NMR: Programs for checking the quality of protein structures solved by NMR. *J Biomol NMR*. 1996;8(4):477-86.
  28. Weng G, Wang E, Wang Z, Liu H, Zhu F, Li D, et al. HawkDock: a web server to predict and analyze the protein-protein complex based on computational docking and MM/GBSA. *Nucleic Acids Res*. 2019;47.
  29. Lopez-Blanco JR, Aliaga JI, Quintana-Orti ES, Chacon P. iMODS: internal coordinates normal mode analysis server. *Nucleic Acids Res*. 2014;42(Web Server issue):W271-6.
  30. Lei Y, Zhao F, Shao J, Li Y, Li S, Chang H, et al. Application of built-in adjuvants for epitope-based vaccines. *Peer J*. 2019;6:e6185.
  31. Momtaz F, Foysal J, Rahman MM, Fotadar R. Design of Epitope Based Vaccine against Shrimp White Spot Syndrome Virus (WSSV) by Targeting the Envelope Proteins: an Immunoinformatic Approach. *Turkish J Fish Aquat Sci*. 2018;19:149-59.
  32. Sanchez-Trincado JL, Gomez-Perosanz M, Reche PA. Fundamentals and Methods for T- and B-Cell Epitope Prediction. *J Immunol Res*. 2017;2017:2680160.
  33. Gaudino SJ, Kumar P. Cross-Talk Between Antigen Presenting Cells and T Cells Impacts Intestinal Homeostasis, Bacterial Infections, and Tumorigenesis. *Front Immunol*. 2019;10:360.
  34. Ho NI, Huis In 't Veld LGM, Raaijmakers TK, Adema GJ. Adjuvants Enhancing Cross-Presentation by Dendritic Cells: The Key to More Effective Vaccines? *Front Immunol*. 2018;9:2874.
  35. Zhao L, Zhang M, Cong H. Advances in the study of HLA-restricted epitope vaccines. *Hum Vaccin Immunother*. 2013;9(12):2566-77.
  36. European centre for disease control. Rapid Risk Assessment: Coronavirus disease 2019(COVID-19) in the EU/EEA and the UK- ninth update. 2020.
  37. Meher PK, Sahu TK, Gahoi S, Rao AR. ir-HSP: Improved Recognition of Heat Shock Proteins, Their Families and Sub-types Based On g-Spaced Di-peptide Features and Support Vector Machine. *Front Genet*. 2017;8:235.
  38. Sharma R, Bayarjargal M, Tsunoda T, Patil A, Sharma A. MoRFPred-plus: Computational Identification of MoRFs in Protein Sequences using Physicochemical Properties and HMM profiles. *J Theor Biol*. 2018;437:9-16.
  39. Goulopoulou S, McCarthy CG, Webb RC. Toll-like Receptors in the Vascular System: Sensing the Dangers Within. *Pharmacol Rev*. 2016;68(1):142-67.
  40. Takeda K, Akira S. Toll-like receptors in innate immunity. *Int Immunol*. 2005;17(1):1-14.
  41. Chen F, Liu H, Sun H, Pan P, Li Y, Li D, et al. Assessing the performance of the MM/PBSA and MM/GBSA methods. 6. Capability to predict protein-protein binding free energies and re-rank binding poses generated by protein-protein docking. *Physical chemistry chemical physics : PCCP*. 2016;18(32):22129-39.
  42. Genheden S, Ryde U. The MM/PBSA and MM/GBSA methods to estimate ligand-binding affinities.

- Expert Opin Drug Discov. 2015;10(5):449-61.
43. Dobbins SE, Lesk VI, Sternberg MJ. Insights into protein flexibility: The relationship between normal modes and conformational change upon protein-protein docking. Proc Natl Acad Sci U S A. 2008;105(30):10390-5.
44. Kovacs JA, Chacon P, Abagyan R. Predictions of protein flexibility: first-order measures. Proteins. 2004;56(4):661-8.
45. Ramakrishna V, Vasilakos JP, Tario JD, Berger MA, Wallace PK, Keler T. Toll-like receptor activation enhances cell-mediated immunity induced by an antibody vaccine targeting human dendritic cells. J Transl Med. 2007;5(1):1-14.